Thruster Loop Controller design of Sun Mode and Maneuver Mode for KOMPSAT-2 (ICCAS 2004)

Hong-Taek Choi.[*], Shi-Hwan Oh[**], and Seung-Wu Rhee[***]

* Korea Aerospace Research Institute, Yusung P.O.Box 113, Daejon, 305-600 Korea
(Tel :+ 82-42-860-2808; E-mail : hongtaek@kari.re.kr)
** Korea Aerospace Research Institute, Yusung P.O.Box 113, Daejon, 305-600 Korea
(Tel : +82-42-860-2446; E-mail : oshwan@kari.re.kr)
*** Korea Aerospace Research Institute, Yusung P.O.Box 113, Daejon, 305-600 Korea
(Tel : +82-42-860-2447; E-mail : srhee@kari.re.kr)

Abstract: In order to successfully develop attitude and orbit control subsystem(AOCS), AOCS engineer performs hardware selection, controller design and analysis, control logic and interface verification on electrical test bed, integrated system test, polarity test, and finally verification on orbit after launching. Attitude and orbit control subsystem for KOMPSAT-2 consists of standby mode, sun mode, maneuver mode, science mode, and power safe mode to stabilize and to control the spacecraft for performing the mission. The sun mode is usually divided into sun point submode, earth search submode and safe hold submode. The maneuver mode is divided into attitude hold submode and △V submode, while the science mode divided into science coarse submode and science fine submode. Moreover, it is added to back-up mode which uses wheels as an actuator for sun mode and maneuver mode. In this paper, we describe the controller design process and the performance of the design results with respect to the sun mode and the maneuver mode based on thrusters as an actuator using on flexible model.

Keywords: Attitude and Orbit Control Subsystem, Pulse Width Modulation, Beginning of Life, End of Life, Proportional –Integral- Derivative

1. INTRODUCTION

In order to successfully develop attitude and orbit control subsystem(AOCS), AOCS engineer performs hardware selection, controller design and analysis, control logic and interface verification on electrical test bed, integrated system test, polarity test, and finally verification on orbit after launching. AOCS for KOMPSAT-2 consists of standby mode, sun mode, maneuver mode, science mode, and power safe mode to stabilize and to control the spacecraft for performing the mission [1].

In general, the mode transition scenario of KOMPSAT-2 is simply described as follows. Standby mode is only ground test mode before separating spacecraft from launch vehicle. In this mode, sensors are activated but actuators are all disabled. After separating from launch vehicle, solar array is deployed. After that, gyros are selected using gyro selection logic. Then, solar array deployment test is performed using selected gyros. The spacecraft enters sun point submode which is solar array normal to the sun to provide battery charge necessary for the spacecraft power. After sun point submode, it enters earth search submode and automatically transition to attitude hold submode to stabilize the spacecraft. Finally, it enters to the science mode to perform the mission. In this paper, we define thruster control requirements, thruster control loop design, the controller design process and the performance of the design results with respect to the sun mode and the maneuver mode based on thrusters as an actuator using on flexible model [2].

2. THRUSTER CONTROL REQUIREMENTS

The stability requirements for the thruster loop design are as follows: The closed loop bandwidth for each axis maintains less than 0.03 Hz to separate from the first natural frequency of spacecraft which is 0.6 Hz. The open loop gain margin for each axis controller design maintains greater than 10 dB with the solar array flexible mode. Finally, the open loop phase margin for each axis controller design maintains greater than 30 degree with the solar array flexible mode.

2.1 Sun Point Submode

In sun point submode, the system successfully orients the solar array normal towards the sun from any initial orientation within 10 minutes in sunlight. The system acquires sun from any attitude with initial rates of 2.0 deg/sec per axis. The steady-state attitude pointing error with respect to the sun line is less than 8 degrees (3σ) to provide the required power of spacecraft for pitch and yaw axis, respectively. The steady-state roll rate control error is less than 0.2 deg/sec (3σ).

2.2 Earth search Submode

In earth search submode, the steady-state attitude pointing error with respect to the sun line is less than 4 degrees (3σ) for a vector normal to the solar panels. The steady-state rate is 2.0 deg/sec$\pm$0.15 deg/sec (3σ) about the solar array normal axis to acquire the earth. The earth capture is completed within one orbit after ground command initiation.

2.3 Safe Hold Submode

In safe hold submode, the system is capable of acquiring the sun with an initial angular momentum of 5.0 N-m-sec per axis. The system successfully orients the solar array normal towards the sun from any initial orientation within 10 minutes in sunlight. The system is capable of remaining sun pointed for 30 days without ground intervention. The steady-state attitude pointing error with respect to the sun line is less than 15 degree (3σ) for a vector normal to the solar panels. The steady-state roll rate control error is less than 0.2 deg/sec (3σ).

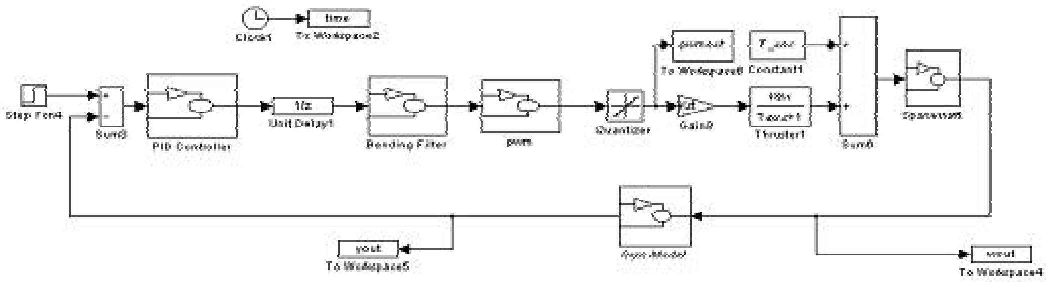

Fig. 1 Single Axis Thruster Control Loop Block Diagram

2.4 Attitude Hold Submode

In attitude hold submode, the steady-state attitude with respect to LVLH attitude during LVLH hold is less than 0.5 degree for each axis when attitude updates are enabled. The steady-state attitude pointing error with respect to the commanded attitude during LVLH hold is less than 1.5 degree for roll/yaw axes and 2.0 deg for pitch axis when attitude updates are enabled. The steady-state attitude pointing error with respect to the commanded attitude during inertial hold or LVLH hold is less than 10.0 degrees for each axis when attitude updates are disabled. The system is capable of reorientation maneuvers up to 180 degrees at rates 1.1 deg/sec in all axes. The system is capable of settling to less than 0.1deg/sec within 5 minutes after the completion of a maneuver.

2.5 Del V Submode

In Del V submode, the steady-state attitude pointing error with respect to the commanded attitude during a Del V burn is less than 3.0 degree (3σ) for all axes. All Del V burns is executed within 5 hours of disabling attitude updates to meet the above steady-state pointing requirements (due to gyro drift). The angular start-up transient error at the beginning of a Del V burn doesn't exceed 10 degrees(3σ) and meets the above pointing requirement in less than 3 minutes.

3. THRUSTER CONTROL LOOP DESIGN

The moment of inertia of spacecraft at BOL is

$$I = \begin{bmatrix} 608.48 & 10.97 & 1.11 \\ -10.97 & 438.92 & 9.64 \\ 1.11 & 9.64 & 408.36 \end{bmatrix} Kg - m^2 \quad (1)$$

Center of mass gravity(C.G.) at BOL is C.G.=[-6.34 -0.58 760.44] mm at BOL from S/C frame. Center of mass gravity at EOL is assumed to more 50.8 mm up along z axis considering the case of KOMPSAT-1. Thus, C.G=[-6.34 -0.58 811.24] mm at EOL from S/C frame. The single axis thruster control loop block diagram is shown in Fig. 1. It consists of single axis S/C dynamics, thruster controller, gyro model and PID controller. The sampling time of thruster controller uses 0.75 second since it is controlled by firing roll-pitch-yaw pluses sequentially in 0.25 sec, respectively. For Del V burn operation, the constant disturbance torque is used to model the thruster disturbance torque uncertainty. Table 1 shows the PWM (pulse width modulation) parameters. The purpose of the PWM is to ensure that a single minimum pulse width firing is used in steady state limit cycle operation of the thruster of the thruster control loop. This ensures that the min. propellant is consumed for steady state operations which is important for extended duration operations(e.g. safe hold 30 day requirements).

Table 1. PWM Parameters

Items	Values
Min. Pulse Width(sec)	0.03
Max. Pulse Width(sec)	0.25
Feedback Gain	0.5

Table 2 shows the parameters which is used in the Gyro Model. The damping coefficient and roll-off frequency of gyro in the block diagram are 0.7 and 10 Hz, respectively.

Table 2. Gyro Quantizer Parameters

Items	Values
Quantizer Resolution	0.2 arcsec/pulse
Rate Saturation Limit	$\pm$7 deg/sec

Thruster torques for each axis is

$$\vec{T} = (\vec{R} - \vec{G}) \times \vec{F} \quad (2)$$

where $\vec{R}$ is the thruster position from the separation plane of spacecraft, $\vec{G}$ is the center of gravity from the separation plane of spacecraft, $\vec{F}$ is thruster force. Thruster force levels at BOL and EOL are the function of fuel pressure levels which are 4.23 N at BOL and 1.05 N at EOL. Thruster torque for each axis at BOL is as follows:

axis	Thruster torque
roll	1.10 N-m
pitch	1.48 N-m
yaw	0.37 N-m

Thruster torque for each axis at EOL is as follows:

axis	Thruster torque
roll	0.27 N-m
pitch	0.37 N-m
yaw	0.09 N-m

It is noticed that thruster torque at EOL is reduced since thruster force is reduced according to the consumption of fuel. The redundant thruster is designed to minimize the effect of thruster torque and the stretching gain exists to control the gain at EOL The proportional gain is obtained using the follow equation as well as considering control bandwidth requirement.

$$K_p \times \theta_{deadzone} = \Delta_{\min.pulse} \quad (4)$$

where $\Delta_{\min.pulse}$ is thruster minimum pulse and $\vartheta_{deadzone}$ is control deadzone. The natural frequency and damping ratio of bending filter is designed enough to get the gain margin and phase margin and separated from the open loop cross over frequency. The differentiator is used to produce damping in the control system and the integrator is used in only Del V burn submode for biasing off constant disturbance torques.

4. FLEXIBLE MODEL

The spacecraft model is derived from finite element method using NASTRAN program [3-4]. The dynamic model is composed of 100 mode and each mode has a natural frequency calculated from physical characteristics and spacecraft configuration. Among them, 20 mode is selected to reduce the calculation time. The followings present the procedure derived ordinary differential equation from spacecraft dynamics in state space. Spacecraft with flexible mode acting on external force F(t), modal damping C can be described by Eq. (5)

$$M\ddot{\underline{q}} + C\dot{\underline{q}} + K\underline{q} = f(t)\underline{e}_i \quad (5)$$

Where M is the mass, K stiffness matrix, q state vector and $\underline{e}_i$ is the location of external force. In order to separate each mode , modal matrix is $\underline{P}$, principal axis is $\underline{p}$,

$$\underline{P}^T M \underline{P}\ddot{\underline{p}} + \underline{P}^T C \underline{P}\dot{\underline{p}} + \underline{P}^T K \underline{P}\,\underline{p} = \underline{P}^T f(t)\underline{e}_i \quad (6)$$

Where modal matrix is $\underline{P} = [P_1/\sqrt{M}\ P_2/\sqrt{M}\ P_3/\sqrt{M}\ \Lambda\,]$. Therfore, if coupled modal damping is small enough, $\underline{P}^T C \underline{P} = diag\{2\xi_1\omega_{n1}, 2\xi_2\omega_{n2}, 2\xi_3\omega_{n3}, \Lambda\}$ $\underline{P}^T K \underline{P} = diag[\omega_{n1}^2, \omega_{n2}^2, \omega_{n3}^2, \Lambda\,]$, $\underline{P}^T \underline{e}_i = \Phi_{ij}$. Then, Eq.(6) is described by

$$\ddot{p}_i + 2\xi_i\omega_{ni}\dot{p}_i + \omega_{ni}^2 p_i = \Phi_{ij} f(t) \quad (7)$$

Spacecraft with flexible model can be expressed for general coordinate in state space by the following Eq.(8)

$$\dot{X} = AX + Bu$$
$$Y = CX + Du \quad (8)$$

Where matrix A, B, C, and D can be described by

$$A = \begin{bmatrix} 0 & I \\ -\omega_n & -2\xi\omega_n \end{bmatrix},$$

$$B = \begin{bmatrix} 0 \\ \Phi^T_{thruster} \end{bmatrix},$$

$$C = \begin{bmatrix} \Phi_{CSSA} & 0 \\ 0 & \Phi_{Gyro} \end{bmatrix},$$

$$D = \begin{bmatrix} 0 \\ 0 \end{bmatrix}$$

Where ϖ_n is natural frequency, ξ is damping ratio, Φ_i is modal matrix at coarse sun sensor, gyro and thrusters and I is unit matrix.

5. CONTROLLER DESIGN RESULTS

The performance of the design results is described with respect to the sun mode and the maneuver mode based on thrusters as an actuator using on flexible model [5-6]. Fig. 2 shows roll axis Bode plot for sun point submode. The gain margin maintains greater than 10 dB and the phase margin maintains greater than 30 degree.

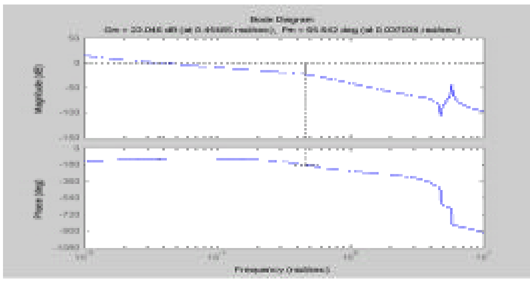

Fig. 2 Bode Plot for Sun Point Submode in Roll Axis @ BOL (Open Loop)

Fig. 3 shows solar array sun point error of sun point submode for pitch and yaw axis when initial angle starts from 0 degree to 180 degree. The settling time is 300 s and the overshoot doesn't appear. The normal vector to the solar array is within 8 degree.

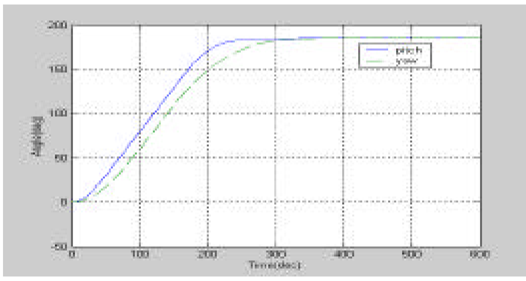

Fig. 3 Solar Array Sun pointing Error of Sun Point Submode(solid : pitch, dashed : yaw)

Table 5 Summary of single Axis Performance Simulation Results for Thruster Control Loops

Simulation Test Case	Initial Conditions			Simulation Results			
Submodes	Axis	Initial/CMD Attitude (deg)	Initial/CMD Angular Rate (deg/sec)	Settling Time (sec)	Peak Error (%)	Steady State Error (deg)	Steady State Roll Rate Error (deg/sec)
Safe Hold Submode	roll	180	0.0	400	0	15	0.15
	Pitch	180	0.0	300	0	15	0.15
	Yaw	180	0.0	300	0	15	0.15
Sun Point Submode	roll	180	0.0	200	0	8	0.15
	Pitch	180	0.0	200	0	8	0.15
	Yaw	180	0.0	500	0	8	0.15
Attitude Hold Submode	roll	180	0.0	200	0	1	0.005
	Pitch	180	0.0	200	0	1.5	0.05
	Yaw	180	0.0	200	0	1	0.01
Del V Submode	roll	0	0.0	300	6.5	0.01	0.01
	Pitch	0	0.0	300	8	0.01	0.01
	Yaw	0	0.0	300	2.5	0.01	0.01

Fig. 4 shows angular rate for sun point submode for pitch and yaw axis. Solar array flexible effect is more related to pitch axis. The maximum angular rate doesn't exceed 1.1 deg/s of controller design limit.

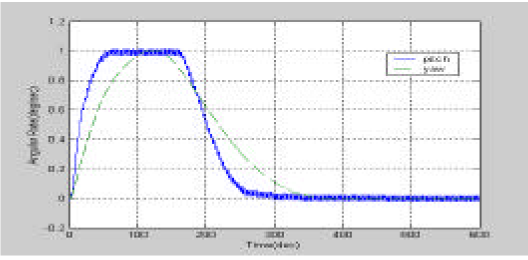

Fig. 4 Angular Rate for Sun point Submode(solid : pitch, dashed : yaw)

Fig. 5 shows pulse width for sun point submode in roll axis. The maximum pulse width is 0.25 s and the minimum pulse width is 0.03 s. The thruster is fired in transient and the thruster is fired to trigger the direction between the deadzone in steady state.

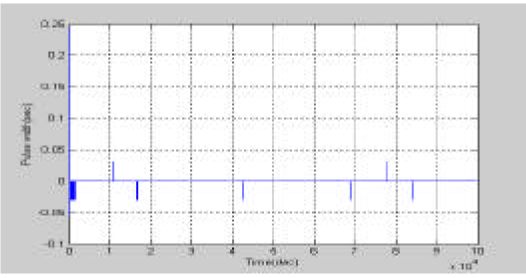

Fig. 5 Pulse Width for Sun point Submode in Roll Axis @ BOL with Flexible Mode

Fig. 6 shows the phase plane for sun point submode in roll axis for 100,000sec. The angle is changed from 174 degree to 186 degree that is satisfied the pointing requirement.

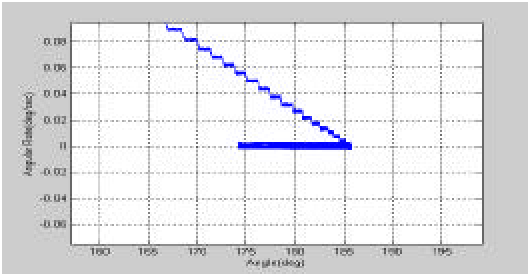

Fig. 6 Phase Plane Plot for Sun point Submode in Roll Axis @ BOL with Flexible Mode

Similar results are obtained to satisfy the design constraints for the other modes. Table 5 is a summary of the single axis performance simulation results for the thruster control loops.

6. CONCLUSIONS

In this paper, we describe the controller design process and the performance of the design results with respect to the sun mode and the maneuver mode based on thrusters as an actuator using on flexible model. The pointing accuracy is satisfied with the design requirements for sun mode and maneuver mode using simulations. These results can be used to design the low earth orbit satellite in future.

REFERENCES

[1] KARI, Subsystem Specification for the Attitude and Orbit Control Subsystem, 2002

[2] S.W. Rhee, "Thruster Loop Design of Flexible Model and Simulation," IOC. KOMPSAT.96.450.051, Dec. 20, 1996

[3] William T. Thomson, Theory of Vibration with Applications, Prentice Hall, 1988

[4] Leonard Meirovitch, Elements of Vibration Analysis, McGraw-Hill, 1986

[5] Wertz, James R., Spacecraft Attitude Determination and Control, D. Reidel Publishing Co., 1986

[6] B. Wie, Spacecraft Dynamics and Control: Application of Dynamical Systems Theory, Arizona State University, 1995, pp. 431-436.